Cent. Eur. J. Phys. • 10(1) • 2012 • 197-205
DOI: 10.2478/s11534-011-0012-9

VERSITA

Central European Journal of **Physics**

The structural, elastic and thermodynamic properties of intermetallic compound $CeGa_2$

Research Article

Yasemin Ö. Çiftci[1]*, Kemal Çolakoğlu[1], Cansu Çoban[2], Engin Deligöz[3]

1 *Gazi University, Department of Physics, Teknik okullar, 06500, Ankara, Turkey*

2 *Balikesir University, Department of Physics, Balikesir, Turkey*

3 *Aksaray University, Department of Physics, 68100, Aksaray, Turkey*

Received 27 July 2010; accepted 26 September 2011

Abstract: The structural, elastic and thermodynamic characteristics of $CeGa_2$ compound in the AlB_2 (space group: P6/mmm) and the omega trigonal (space group: P-3m1) type structures are investigated using the methods of density functional theory within the generalized gradient approximation (GGA). The thermodynamic properties of the considered structures are obtained through the quasi-harmonic Debye model. The results on the basic physical parameters, such as the lattice constant, the bulk modulus, the pressure derivative of bulk modulus, the phase-transition pressure (P_t) from P6/mmm to P-3m1 structure, the second-order elastic constants, Zener anisotropy factor, Poisson's ratio, Young's modulus, and the isotropic shear modulus are presented. In order to gain further information, the pressure and temperature-dependent behavior of the volume, the bulk modulus, the thermal expansion coefficient, the heat capacity, the entropy, Debye temperature and Grüneisen parameter are also evaluated over a pressure range of 0-6 GPa and a wide temperature range of 0-1800 K. The obtained results are in agreement with the available experimental and the other theoretical values.

PACS (2008): 71.15.Mb; 67.25.de; 62.20.de; 64.60.-i

Keywords: phase transition pressure • elastic properties • thermodynamic properties

1. Introduction

The rare-earth intermetallic compound cerium di-gallide crystallizes in the AlB_2 - type structure at ambient conditions with the space group symmetry P6/mmm [1–5]. Several similar systems exhibiting the AlB_2-type structure was investigated by Chandra Shekar et al. [1–3]. They found that these systems have a tendency to follow a sepecific structural sequence under pressure, namely AlB_2 (P6/mmm) to $ZrSi_2$ (Cmcm) to $ThSi_2$ ($I4_1/amd$) to Cu_2Sb (P4/nmm) type, by using X-ray diffraction techniques. They have also reported the lattice constants ($a = 4.298 \pm 0.001$ Å and $c = 4.334 \pm 0.001$ Å) and the phase transition pressure (~ 16 GPa) obtained exper-

*E-mail: yasemin@gazi.edu.tr

imentally [4] for $CeGa_2$. Rajagopalan et al. [5] studied the electronic structure and structural phase transition from AlB_2 to P-3m1 structure using the tight-binding linear muffin-tin orbital (TB-LMTO) method. Magnetic ordering and indirect exchange interactions were studied in the series of rare-earth intermetalic compounds RGa_2 (R=Ce, Pr, Nd, Gd, Tb, Dy, Ho and Er) by Tsai et al. [6]. Umehara et al. have measured the de Haas-van Alphen (dHvA) effect and magnetoresistance of the ferromagnetic $CeGa_2$ in the hexogonal structure [7]. The measurements of the electrical resistivity, Hall effect, magnetoresistance and thermoelectric power for RGa_2 (R=La, Ce and Sm) single crystals are presented by Henmi et al. [8].

Although a few experimental and theoretical works are present on the $CeGa_2$ compounds, to our knowledge, the data does not deal with the mechanical and thermodynamical properties of $CeGa_2$. The present work aims to cover these properties.

2. Method of calculation

All calculations have been carried out using the Vienna Ab initio Simulation Package (VASP) [9–13] based on the density functional theory (DFT). VASP is a package for performing the ab-initio quantum-mechanical molecular dynamics (MD) simulations using Pseudopotentials or PAW and plane waves basis set. The atomic number and the atomic positions of the considered material, which are known, are the only input parameters in these calculations. In VASP, the Kohn-Sham equations are solved self consistently with an iterative matrix diagonalisation and the Pulay/Broyden [14, 15] mixing method for the charge density. Combining these two techniques makes the code very efficient, especially for transition metal systems. The interaction between ions and electrons is described by the ultra-soft Vanderbilt pseudopotential (US-PP) or by the projector-augmented wave (PAW) method [16, 17]. US-PP (and the PAW methods) allow for a considerable reduction of the number of plane-waves per atom. Besides the pure local density (LDA), several gradient-corrected functions are implemented in VASP to account for the non-local Exchange correlation (BP, PW91, PBE). The number of K-points in the irreducible part of the Brillouin zone has a great influence on the accuracy of the calculations. This makes it clear that the sampling set should be chosen very carefully. The K-points sample is usually calculated by the program using the Monkhorst-Pack method [18]. The algorithms implemented in VASP are based on either the conjugate gradient scheme, the block Davidson scheme or a residual minimization scheme (RMM). These algorithms calculate the forces and electronic ground state for a given geometry in a few iterations. These steps are then repeated until an energy criterion is ignored and only the forces are minimized. The gradient-corrected functionals in the form of the generalized-gradient approximation (GGA) by Perdew and Wang [19, 20] have been used. The projector-augmented wave (PAW) method developed by Blöchl [21] provided by VASP to describe the interactions between ions and electrons is used. All results presented below have been obtained by using a plane wave basis with an energy cutoff of 650 eV. The k-points of $14\times14\times14$ have been generated by the Monkhorst and Pack [22] grid for the sampling of the Brillouin zone.

The quasi-harmonic Debye model [23–26]] has been applied to calculate the thermodynamic properties of $CeGa_2$ compound. In this model, the non-equilibrium Gibbs function $G^*(V;P,T)$ can be written as [23]

$$G^*(V;P,T) = E(V) + PV + A_{vib}\left[\Theta(V);T\right], \qquad (1)$$

where $E(V)$ is the total energy per unit cell of $CeGa_2$, PV is the constant hydrostatic pressure condition, $\Theta(V)$ is the Debye temperature and Avib is the vibrational Helmholtz free energy which can be written as [27–30]

$$A_{vib}(\Theta,T) = nkT\left[\frac{9\Theta}{8T} + 3\ln\left(1-e^{-\Theta/T}\right) - D(\Theta/T)\right], \qquad (2)$$

where n is the number of atoms per formula unit, and $D(\Theta/T)$ represents the Debye integral. The Debye temperature Θ is expressed as [30]

$$\Theta = \frac{\hbar}{k}\left[6\pi^2V^{1/2}n\right]^{1/3} f(\sigma)\sqrt{\frac{B_s}{M}}, \qquad (3)$$

where M is the molecular mass per unit cell and B_S is the adiabatic bulk modulus which is approximated by the static compressibility as [23]

$$B_s \approx B(V) = V\left[\frac{d^2E(V)}{dV^2}\right], \qquad (4)$$

$f(\sigma)$ is given by [28, 29]

$$f(\sigma) = \left\{3\left[2\left(\frac{2}{3}\frac{1+\sigma}{1-2\sigma}\right)^{3/2} + \left(\frac{1}{3}\frac{1+\sigma}{1-\sigma}\right)^{3/2}\right]^{-1}\right\}^{1/3}, \qquad (5)$$

where σ is the Poisson ratio. Therefore, the nonequilibrium Gibbs function $G^*(V;P,T)$ as a function of $(V;P,T)$ can be minimized with respect to volume V as

$$\left[\frac{\partial G^*(V;P,T)}{\partial V}\right]_{P,T} = 0. \qquad (6)$$

The thermal equation-of-state (EOS) $V(P, T)$ can be obtained by solving the equation (6). The isothermal bulk modulus B_T is given by [23]

$$B_T(P, T) = V\left(\frac{\partial^2 G^*(V; P, T)}{\partial V^2}\right)_{P,T}. \quad (7)$$

The thermodynamic quantities, e.g., heat capacities C_V at constant volume and C_P at constant pressure and entropy S, have been calculated by applying the following relations [23]:

$$C_v = 3nk\left[4D(\Theta/T) - \frac{3\Theta/T}{e^{\Theta/T} - 1}\right], \quad (8)$$

$$C_P = C_V(1 + \alpha\gamma T), \quad (9)$$

$$S = nk\left[4D(\Theta/T) - 3\ln\left(1 - e^{-\Theta/T}\right)\right], \quad (10)$$

where α is the thermal expansion coefficient and is the Grüneisen parameter, which are given by [23]

$$\alpha = \frac{\gamma C_v}{B_T V}, \quad (11)$$

$$\gamma = -\frac{d\ln\Theta(V)}{d\ln(V)}. \quad (12)$$

3. Results and discussion

3.1. Structural and electronic properties

We have computed the equilibrium lattice constant, the bulk modulus, and its pressure derivative by minimizing the total energy for the P6/mmm and P-3m1 structures of the $CeGa_2$ crystal calculated at different volumes by means of Murnaghan's equation of state [31] as shown in Fig. 1. From the Fig. 1, it can be clearly seen that the P6/mmm structure of $CeGa_2$ is more stable than the P-3m1 phase. Optimized lattice constants, presented in Table 1 with the experimental values taken from [4] and [32] for $CeGa_2$, are found to be $a = 4.243$ Å $c = 4.353$ Å for the P6/mmm structure and $a = 4.628$ Å, $c = 3.436$ Å for the P-3m1 structure, respectively. These results are close to the values of experimental data given in Table 1. The computed bulk modulus and its pressure derivative are also listed in Table 1 for the P6/mmm (67.55 GPa) and P-3m1 structures (67.215 GPa) of $CeGa_2$. Our results are very close to each other for both phases, but its value for the P6/mmm structure is lower (about 9%) from the experimental result in [4]. The phase transition behavior of this compound is also investigated to see the high pressure structural properties. The total energy curves for $CeGa_2$ in two different crystal structures are shown in Fig. 1. It is clear from the Fig. 1 that $CeGa_2$ compound undergoes a phase transition from P6/mmm to P-3m1 structure. These transition pressures (Pt) are determined by calculating the Gibb's free energies at 0 K. The related enthalpy changes (ΔH)-pressure (P) graphs are plotted for both phases for $CeGa_2$ compound as shown in Fig. 2. The transition pressure is a pressure at which $H - P$ curves for both phases cross. In the present case, the phase transition in $CeGa_2$ occurs from P6/mmm to P-3m1 structure at about 7.5 GPa, and our value is about 46% lower than the experimental (~ 16 GPa) value in Ref. [4] and is very far from the theoretical value (~ 30.6 GPa)

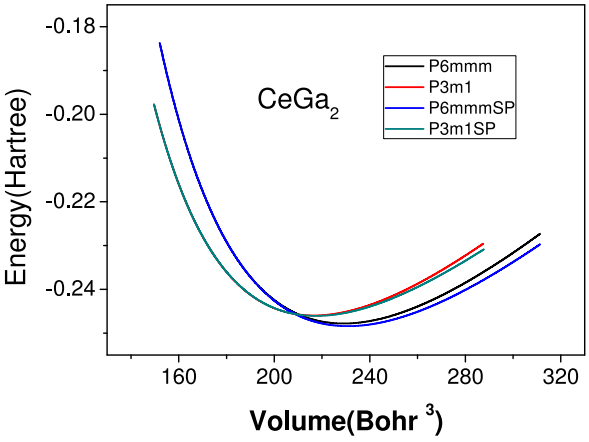

Figure 1. Energy versus volume curves with and without spin polarized (SP) for two different crystal structures of $CeGa_2$ compounds.

Table 1. Calculated equilibrium lattice parameters(a_0, c), bulk modulus (B), pressure derivatives of bulk modulus (B') , formation energies (ΔH), debye temperature (Θ) and other theoretical and experimental values for $CeGa_2$ compound.

Material	Ref.	a Å	c Å	B (GPa)	B'	ΔH (eV/atom)	Θ (K)
$CeGa_2$ (P6/mmm)	Present	4.243	4.353	67.55	4.227	-3.43	346.43
	Exp. [4]	4.298 ±0.001	4.334 ±0.001	72 ±12	4 ± 1		
	Exp. [28]	4.285	4.340				
	Theory [5]			96.74			
$CeGa_2$ (P-3m1)	Present	4.628	3.436	67.22	4.37	-3.41	313.86

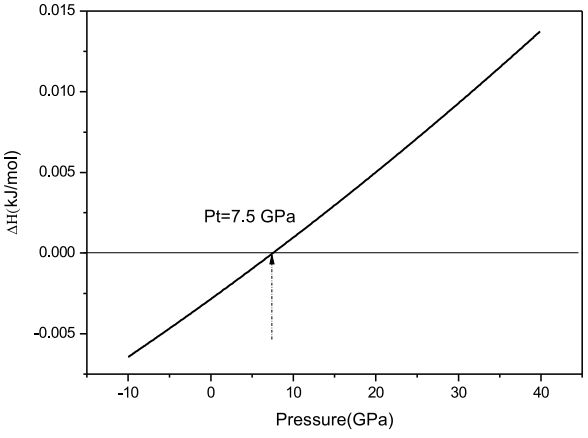

Figure 2. Estimation of phase transition pressure from P6/mmm to P-3m1 structure for $CeGa_2$.

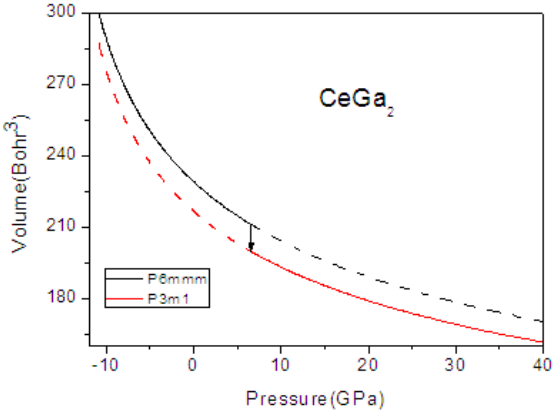

Figure 3. Volume versus pressure curves for from P6/mmm to P-3m1 structures of $CeGa_2$.

in Ref. [5]. The present result is also verified in terms of the "common tangent technique" in Fig. 1 and the same value of 7.5 GPa is obtained. These large deviations on P_t should shed light on the other experimental works. The volume-pressure curves are plotted for the P6/mmm and P-3m1 phases of this compound (see Fig. 3). The cell volume with both crystal phases decreases with increasing pressure. The discontinuity in volume takes place at the phase transition pressure. At around 7.5 GPa, $CeGa_2$ undergoes a structural phase transition to P-3m1 from P6/mmm structure type with a volume collapse of 5.4%, which is in good agreement with the experimental value (6%) [5]. The calculated value of the formation energy for both P6/mmm (-3.43 eV) P-3m1 (-3.41 eV) phases implies that the P6/mmm structure is more stable than P-3m1, and can be synthesized more easily. The present value of the Debye temperature (see Table 1) for P6/mmm and P-3m1 phases are found to be 346.43 K and 313.86 K, respectively.

Table 2. Elastic constants (in GPa) at 0 GPa pressure for $CeGa_2$.

Material	Ref.	C_{11}	C_{12}	C_{13}	C_{33}	C_{44}	C_{66}
$CeGa_2$ (P6/mmm)	Present	172.82	29.62	36.79	89.40	71.59	61.12
$CeGa_2$ (P-3m1)	Present	128.47	47.07	52.72	83.06	40.70	69.74

Due to the magnetic nature of Ce-containing compounds, the magnetic ordering of $CeGa_2$ was taken into account by means of the spin-polarized calculations. We have computed the total energy with and without the spin-polarization (ferromagnetic ordering) cases for both phases in Fig. 1. Our results show that while spin-polarization slightly affects the total energy of P6/mmm phase at higher volumes, no significant difference was found between spin-polarized and non-spin polarized energies for P-3m1 phase at lower volumes. We therefore neglected the spin polarization effects in the mechanical and thermodynamical calculations.

The calculated total density of states (DOS) for spin up/down cases are shown in Fig. 4 The fermi level (E_f) is set to zero energy. It can be seen that there are some bands crossing the Fermi level, which indicates the metallic behaviour of P6mmm structure of $CeGa_2$. The metallic character of $CeGa_2$ is confirmed by analysis of the DOS. The calculated total magnetic moments in μB for $CeGa_2$ is 0.75, which is significantly lower than the experimental value of 1.4 μB [33].

3.2. Elastic properties

Elastic constants are important properties of solids which determine the elasticity, the mechanical stability and the stiffness of crystals. A study of the elastic properties of materials is essential to understand the chemical bonding and cohesion [34]. In this study, the second-order elastic constants, presented in Table 2, have been calculated using the "stres-strain" relations [35]. The known conditions for the mechanical stability of a hexagonal crystal are: $C_{11} > 0, C_{11} - C_{12} > 0, (C_{11} + C_{12})C_{33} - 2C_{12} > 0$. Our results presented in Table 2 satisfy these stability conditions for both phases of $CeGa_2$. To our knowledge, there is no available data for elastic constants to compare with the present results. The pressure-dependent behaviours of the second-order elastic constants are also presented (see Fig. 5 a, b) for both phases P6/mmm and

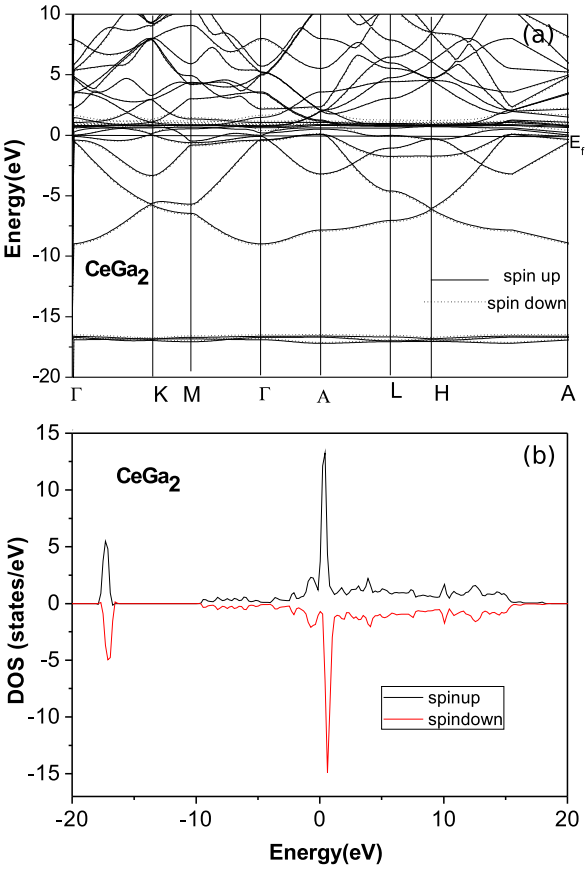

Figure 4. (a) Calculated band structures and (b) DOS with spin polarized case for P6/mmm structure of $CeGa_2$.

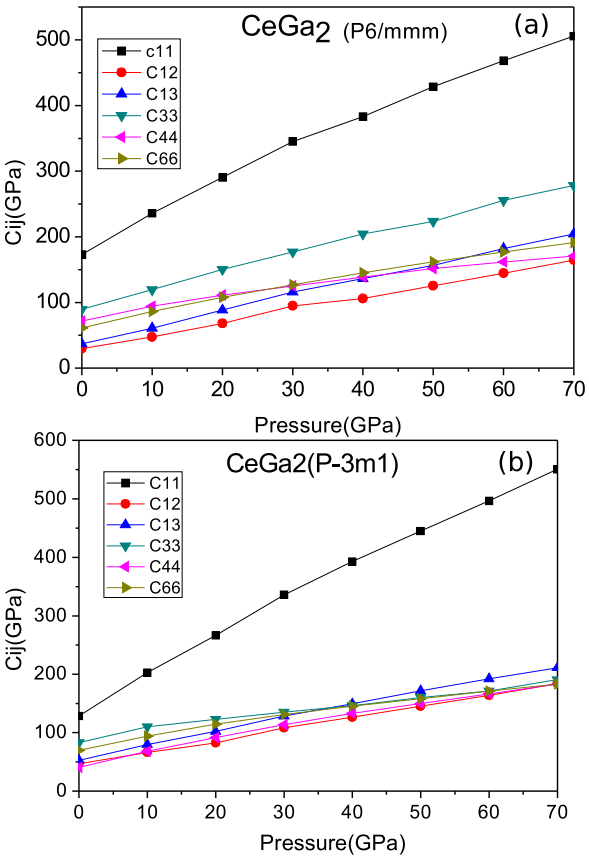

Figure 5. The variation of second-order elastic constants (C_{ij}) with pressure for (a) P6/mmm (b) P-3m1 structures of $CeGa_2$.

P-3m1 of $CeGa_2$. As expected, C_{ijs} increases almost monotonically with pressure up to the considered pressure (70 GPa). For the investigation of their hardness, the elastic properties e.g., the Zener anisotropy factor (A), Poisson's ratio (ν) Young's modulus (E), are often measured for polycrystalline materials. The Zener anisotropy factor A is calculated using the relation [36]

$$A = \frac{2C_{44}}{C_{11} - C_{12}}. \tag{13}$$

Poisson's ratio ν, and Young's modulus E are calculated in terms of computed data by using the following relations [37]:

$$\nu = \frac{1}{2}\left[\frac{B - \frac{2}{3}G}{B + \frac{1}{3}G}\right], \tag{14}$$

and

$$E = \frac{9GB}{G + 3B}, \tag{15}$$

where $G = (G_V + G_R)/2$ is the isotropic shear modulus, G_V is the Voigt's shear modulus corresponding to the upper bound of G values, and G_R is the Reuss's shear modulus corresponding to the lower bound of G values; they can be written as:

$$\begin{aligned} B_V &= (1/9)\left[2\left(C_{11} + C_{12}\right) + 4C_{13} + C_{33}\right] \\ G_V &= (1/30)\left[M + 12C_{44} + 12C_{66}\right] \\ B_R &= C^2/M \\ G_R &= (5/2)\left[C^2 C_{44} C_{66}\right] / \left[3B_V C_{44} C_{66}\right. \\ &\left. + C^2\left(C_{44} + C_{66}\right)\right] \\ M &= C_{11} + C_{12} + 2C_{33} - 4C13 \\ C^2 &= \left(C_{11} + C_{12}\right) C_{33} = 2C_{13}^{2'}. \end{aligned} \tag{16}$$

The calculated Zener anisotropy factor A, Poisson's ratio ν, Young's modulus E, and the isotropic shear modulus G and G/B for $CeGa_2$ are given in Table 3.

The Zener anisotropy factor A is a measure of the degree of elastic anisotropy in solids. The A takes the value of 1 for a completely isotropic material. If the value of A is smaller or greater than unity, it shows the degree

Table 3. The calculated Zener anisotropy factor A, Poisson's ratio ν, Young's modulus E, and isotropic shear modulus G and G/B for $CeGa_2$.

Material	Ref.	A	ν	E(GPa)	G(GPa)	G/B
$CeGa_2$(P6/mmm)	Present	0.99	0.16	136.99	58.71	0.86
$CeGa_2$(P- 3m1)	Present	1.00	0.24	109.62	44.19	0.63

of elastic anisotropy. The calculated Zener anisotropy factors for the P6/mmm and P-3m1 structures of $CeGa_2$ are equal to 1, which indicates that these compounds are completely isotropic materials.

The Poisson's ratio ν and Young's modulus E are very important properties for industrial applications. The Poisson's ratio ν provides more information about the characteristics of the bonding forces than any of the other elastic constants. The lower limit and upper limit of Poisson's ratio ν are 0.25 and 0.5 for central forces in solids, respectively [38]. Calculated ν values are equal to 0.16 and 0.24 for the P6/mmm and P-3m1 structures of $CeGa_2$, respectively. It shows that the interatomic forces in the $CeGa_2$ are not predominantly central forces. The Young's modulus E, which is the ratio between stress and strain, is required to provide information about the measure of the stiffness of solids. The present values of Young's moduli decrease from P6/mmm to P-3m1, which points out that the P6/mmm structure of $CeGa_2$ is stiffer than the P-3m1 structure of $CeGa_2$.

The bulk modulus is a measure of resistance to volume change by applied pressure, whereas the shear modulus is a measure of resistance to reversible deformations due to shear stress [39]. Therefore, by using the isotropic shear modulus, the hardness of a material can be determined more accurately than by using the bulk modulus. The calculated isotropic shear modulus decreases from P6/mmm to P-3m1 structure. We can conclude that the P-3m1 is softer than the P6/mmm structure of $CeGa_2$, which agrees with the results as previously noted in the paragraph related to Young's modulus E. The other commonly used empirical relations between bulk and isotropic shear modulus for covalent and ionic materials on their brittle/ductile behavior are $G \sim 1.1B$ and $G \sim 0.6B$, respectively [40, 41]. The present values of G/B are 0.85 (P6/mmm) and 0.62 (P-3m1), and they are higher than the critical value of 0.5. These results also support their ionic and brittle character. According to this G/B criterion, the P6/mmm structure of $CeGa_2$ is more brittle than the P-3m1 structure of the same compound.

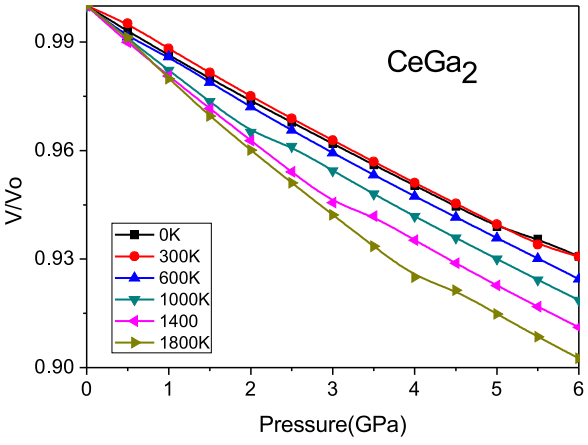

Figure 6. The variations of volume with the pressure at different temperatures for P6/mmm structure of $CeGa_2$.

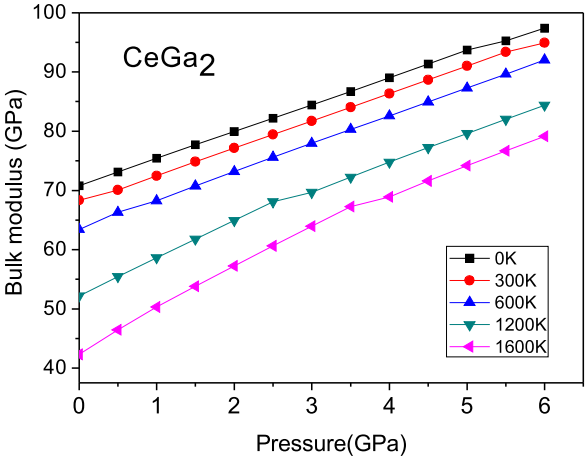

Figure 7. The variations of bulk modulus with the pressure for different temperature of $CeGa_2$.

3.3. Thermodynamic properties

The thermal properties are determined in the temperature range from 0 to 1800 K for the more stable structure (P6/mmm structure) of $CeGa_2$, where the quasi-harmonic Debye model remains fully valid. The pressure effect is studied in 0-6 GPa range. The relationships between volume and pressure at different temperatures are shown in Fig. 6 for $CeGa_2$. It is seen that when the pressure increases from 0 GPa to 6 GPa, the volume decreases. The reason for this change can be attributed to the atoms in the interlayer which become closer and whose interactions become stronger. For this compound, the volume increases with increasing temperature but the rate of increase is very moderate. The variation of the bulk modulus with pressure at different temperatures is shown in Fig.

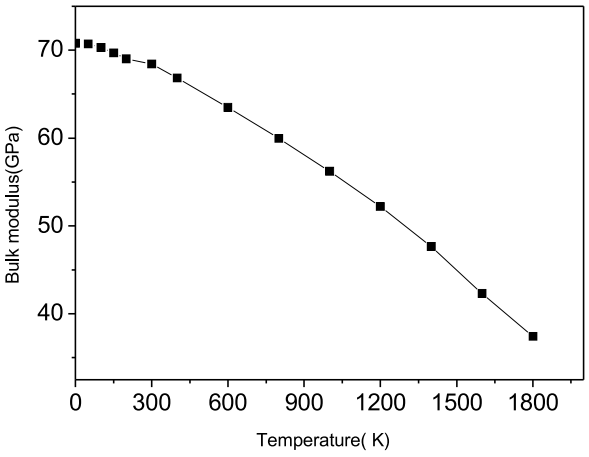

Figure 8. The variation of bulk modulus (B) with temperature at $P = 0$ GPa for $CeGa_2$.

7. for $CeGa_2$. It can be seen that bulk modulus decreases with the temperature at a given pressure and increases with pressure at a given temperature. The temperature-dependent behavior of the bulk modulus is also investigated up to 1800 K and the obtained results are plotted in Fig. 8. The third-order polynomial fitting gives the following equation:

$$B_{(T)} = 71.029 - 0.00773T - 8.14284E - 6T^2 + 1.1502E - 9T^3\,;\ T < 1800\ K. \quad (17)$$

The value of the bulk modulus (~71 GPa) from the fitting procedure at $P = 0$ GPa at $T = 0$ K is close to our previous result in Table 1 and is in excellent agreement with the experimental value of 72 ± 12 GPa by Chandra Shekar [4]. The calculated properties at different temperatures are very sensitive to the vibrational modes. In the quasi-harmonic Debye model, the Grüneisen parameter $\gamma(T)$ nd the Debye temperature $\Theta(T)$ are two key quantities. These quantities at various temperatures (0, 400, 800,1200,1600,2000 K) and different pressures (0, 1, 2, 3, 4, 5 and 6 GPa) are calculated and shown in Table 4 for $CeGa_2$ compound. It is clear from Table 4 that as the temperature increases, the Grüneisen parameter decreases and the Debye temperature increases. The temperature-dependent behavior of the constant-volume heat capacity, C_v , and the constant pressure heat capacity, C_p, at different pressures P are shown in Fig. 9(a,b) for $CeGa_2$ in stable phase. It is seen that both curves exhibit a similar trend, but the values of C_p, as expected, are slightly higher than that for C_v at higher temperatures. It is seen from Fig. 9(a) that when T¡ 300 K, C_v increases very rapidly with temperature; when $T >$ 400 K, C_v increases slowly with

Table 4. The calculated Debye temperature Θ (K) and Grüneisen parameter γ (K) over a wide range of temperatures and pressures of $CeGa_2$ compound.

	P (GPa)						
T (K)	0	1	2	3	4	5	6
0 Θ	346.43	356.79	366.61	376.06	385.44	394.78	401.68
400 Θ	339.61	349.13	359.46	369.24	378.73	388.18	397.59
800Θ	326.04	339.22	348.81	359.22	378.73	378.59	388.08
1200Θ	311.48	325.18	338.65	348.33	358.83	368.73	378.30
1600Θ	294.23	310.18	324.25	338.01	347.80	358.40	368.36
1800Θ	286.66	301.67	316.74	330.73	344.57	352.95	363.25
0γ	2.179	2.130	2.088	2.050	2.014	1.981	1.958
400γ	2.213	2.166	2.118	2.077	2.040	2.005	1.972
800γ	2.287	2.215	2.167	2.119	2.078	2.040	2.005
1200γ	2.378	2.292	2.218	2.169	2.121	2.079	2.041
1600γ	2.505	2.387	2.298	2.221	2.172	2.123	2.081
1800γ	2.570	2.448	2.344	2.260	2.188	2.148	2.102

temperature and it almost approaches a constant called as Dulong-Petit limit ($Cv(T)$ $3R$ for mono atomic solids) at higher temperatures for $CeGa_2$ compound. The variations of the thermal expansion α with temperature at different pressure are given in Fig. 10 for $CeGa_2$ compound. It is seen that the thermal expansion coefficient α also rapidly increases with T at lower temperatures and gradually approaches to a linear increase at higher temperatures. This increasing in α is more rapid at high pressures. Moreover, it is clearly seen that the thermal expansion coefficient decreases with the increasing pressure.

4. Summary and conclusion

In summary, the first principles calculations have been performed to obtain the structural, elastic and thermodynamic properties of $CeGa_2$ compound. The structural parameters (the lattice parameters and bulk modulus) are in good agreement with the previous experimental data. Our results for the elastic constants satisfy the traditional mechanical stability conditions for both phases of $CeGa_2$ compound. The other mechanical data such as Zener anisotropy factor (A), Poisson's ratio (ν), Young's modulus (E), isotropic shear modulus (G) are determined for the first time. The predicted value of the phase transition pressure (7.5 GPa) from P6/mmm to P-3m1 structure is significantly different from the other available findings. Some basic thermodynamical quantities such as the heat capacity (C_v), the thermal expansion (α) coefficient, Grüneisen parameter (γ), and Debye temperature (Θ_D) are calculated based on the quasi-harmonic Debye model at

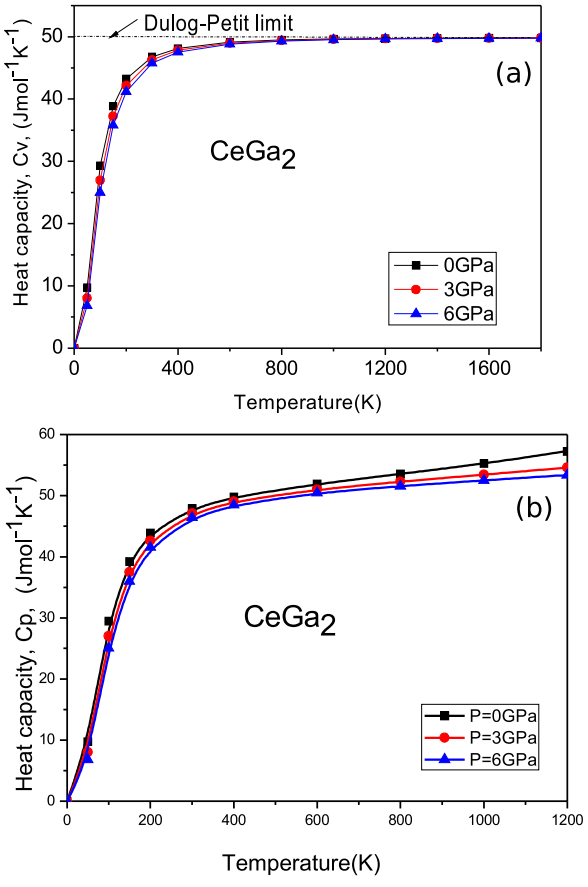

Figure 9. The variations of (a) C_v and (b) C_p with temperature at different pressures for $CeGa_2$.

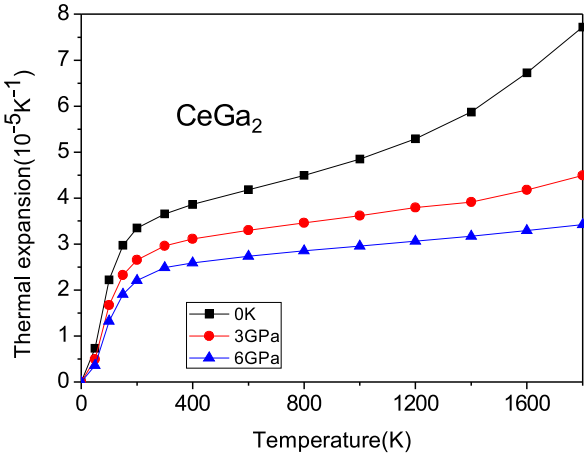

Figure 10. The variation of thermal expansion coefficient with temperature at different pressure of $CeGa_2$.

various temperatures and pressures, and the results are interpreted.

References

[1] P. C. Sahu, N. V. C. Shekar, Pramana 54, 685 (2000)
[2] N. V. C. Shekar, P. C. Sahu, M. Yousuf, K. G. Rajan, Phys. Rev. B 55, 745 (1997)
[3] N. V. C Shekar, P. C. Sahu, M. Yousuf, K. G. Rajan, M. Rajagopalan, Solid State Commun. 111, 529 (1999)
[4] N. V. C. Shekar, N. Subramanian, N. R. S. Kumar, P. C. Suhu, Phys. Status Solidi B 241, 2893 (2004)
[5] M. Rajagopalan, N V. C. Shekar, P. C. Sahu, Physica B 355, 59 (2005)
[6] T. H. Tsai, D. J. Sellmyer, Phys. Rev. B 11, 4577 (1979)
[7] I. Umehera, N. Nagai, Y. Önuki, J. Phys. Soc. Jpn., 60, 1464 (1991)
[8] H. Henmi, Y. A. Oki, T. Fukuhara, I. Sakamoto, H. Sato, Physica B 186, 655 (1993)
[9] G. Kresse, J. Hafner, Phys. Rev. B 47, 558 (1993)
[10] G. Kresse, J. Hafner, J. Phys. Condens. Mat. 6, 8245 (1994)
[11] G. Kresse, J. Hafner, Phys. Rev. B 49, 14251 (1994)
[12] G. Kresse, J. Furthmüller, Comp. Mater. Sci. 6, 15 (1996)
[13] G. Kresse, J. Furthmüller, Phys. Rev. B 54, 11169 (1996)
[14] P. Pulay, Chem. Phys. Lett. 73, 393 (1980)
[15] D. D. Johnson, Phys. Rev. B 38, 12087 (1988)
[16] D. Vanderbilt, Phys. Rev. B 41, 7892 (1990)
[17] P. E. Blochl, Phys. Rev. B 50, 17953 (1994)
[18] H. J. Monkhorst, J. D. Pack, Phys. Rev. B 13, 5188 (1976)
[19] J. P. Perdew, Y. Wang, Phys. Rev. B 45 13244 (1992)
[20] J. P. Perdew et al., Phys. Rev. B 46, 6671 (1992)
[21] P. E. Blöchl, Phys. Rev. B 50, 17953 (1994)
[22] H. J. Monkhorst, J. D. Pack, Phys. Rev. B 13, 5188 (1976)
[23] M. A. Blanco, E. Francisco, V. Luaña, Comput. Phys. Commun. 158, 57 (2004)
[24] F. Peng, H. Z. Fu, X. L. Cheng, Physica B 400, 83 (2007)
[25] F. Peng, H. Z. Fu, X. D. Yang, Solid State Commun. 145, 91 (2008)
[26] F. Peng, H. Z. Fu, X. D. Yang, Physica B 403, 2851 (2008)
[27] M. A. Blanco, A. M. Pendás, E. Francisco, J. M. Recio, R. Franco, J. Mol. Struct.-Theochem 368, 245 (1996)
[28] E. Francisco, J. M. Recio, M. A. Blanco, A. M. Pendás, J. Phys. Chem. 102, 1595 (1998)
[29] E. Francisco, M. A. Blanco, G. Sanjurjo, Phys. Rev. B

63, 094107 (2001)
[30] M. Flórez, J. M. Recio, E. Francisco, M. A. Blanco, A. M. PendÃąs, Phys. Rev. B 66, 144112 (2002)
[31] F. D. Murnaghan, P. Natl. Acad. Sci. USA 30, 244 (1944)
[32] Y. Grin, P. Rogl, B. Chevalier, A. O. Fedorchuk, I. A. Gryhiv, J. Less-Common Met. 167, 365 (1991)
[33] R. D. Dos Reis et al., J. Phys.-Condens. Mat. 22, 486002 (2010)
[34] C. Dong, C. Jing-Dong, Z. Li-Hua, W. Chun-Lei, Y. Ben-Hai, S. De-Heng, Chinese Phys. B 18, 738 (2009)
[35] O. H. Nielson, R. M. Martin, Phys. Rev. Lett. 50, 697 (1983)
[36] C. Zener, Elasticity and anelasticity in metals (University of Chicago Press, Chicago, 1948)
[37] B. Mayer et al., Intermetallics 11, 23 (2003)
[38] H. Fu, D. Li, F. Peng, T. Gao, X. Cheng, Comp. Mater. Sci. 44, 774 (2008)
[39] A. F. Young, C. Sanloup, E. Gregoryanz, S. Scandolo, R. E. Hemley, H. K. Mao, Phys. Rev. Lett. 96, 155501 (2006)
[40] S. F. Pugh, Philos. Mag. 45, 833 (1954)
[41] V. V. Bannikov, I. R. Shein, A. L. Ivanovskii, Phys Status Solidi 1, 89 (2007)